

# Novel Bifunctional Zn–Sn Composite Oxide Catalyst for the Selective Synthesis of Glycerol Carbonate by Carbonylation of Glycerol with Urea

Pandian Manjunathan,<sup>[a]</sup> Raman Ravishankar,<sup>[b]</sup> and Ganapati V. Shanbhag<sup>\*[a]</sup>

A novel Zn–Sn composite oxide is reported as a solid bifunctional catalyst for glycerol carbonylation to give glycerol carbonate in high yields. It was prepared by coprecipitation, solid-state and evaporation methods. Physico-chemical properties of the catalysts were investigated by XRD, N<sub>2</sub> sorption, temperature-programmed desorption, SEM, and TEM techniques. Coprecipitation was found to be better than the other two methods for carbonylation of glycerol. Higher activity of the catalyst was attributed to a high amount of active sites. A series of Zn–

Sn composite oxides with different metal contents and effect of calcination on glycerol carbonate synthesis were also studied. The correlation of activity with total active sites of the catalyst was obtained. Zn–Sn composite catalyst with Zn/Sn molar ratio = 2:1 calcined at 600 °C exhibited 96.0% glycerol conversion with 99.6% selectivity towards glycerol carbonate under optimized reaction conditions. The catalyst was recycled four times with a marginal decrease in activity.

## Introduction

Biofuels derived from the sustainable biomass sources have the potential to displace nonrenewable fossil fuels. Among them, biodiesel has gained much attention from the researchers and its production increased greatly in recent years. Glycerol (1,2,3-propanetriol) is an important byproduct produced (10 wt% referred to the amount of biodiesel) during the synthesis of biodiesel by transesterification of oils and fats. Consequently, the transformation of glycerol into value-added products has stimulated a thirst among the researchers. It made a window of opportunity to transform glycerol into value-added products through various chemical routes such as esterification, etherification, acetalization, transesterification, carbonylation, dehydration and hydrogenation. The products obtained from these processes are glycerol acetins, glycerol ethers, solketal, glycerol carbonate, acrolein, 1,2-propanediol, and 1,3-propandiol. Because of its diverse applications, the synthesis of glycerol carbonate has been considered an attractive process.<sup>[1–5]</sup> Hence, the design of green and chemoselective catalysts for these processes is of great interest.

Glycerol carbonate has both direct and indirect applications in various fields thanks to its interesting properties that lie in between cyclic alkylene carbonate and glycerol. The direct ap-

plications are as biobased solvent, as electrolyte in lithium ion batteries, curing agent, as liquid membrane in gas separation, blowing agent, detergent, and in cosmetics. Indirectly, glycerol carbonate finds application in the synthesis of surfactants, chemical intermediates, and polymers. Glycerol carbonate can be synthesized by different routes, namely, reaction of glycerol with phosgene, transesterification of glycerol with alkyl carbonate, carbonylation of glycerol by urea, and reaction of glycerol with carbon dioxide.

The use of phosgene as a carbonylating agent is inadequate because of its high toxicity and environmentally unfriendly nature. The utilization of carbon dioxide is one among the best processes to obtain glycerol carbonate, but the activation of CO<sub>2</sub> requires severe reaction conditions such as high temperature and pressure. Nevertheless, the process produces minimal yield of glycerol carbonate. The reaction of glycerol with alkyl carbonate by transesterification is an attractive approach to synthesize glycerol carbonate. However, high mole ratio of alkyl carbonate is required to get high yield of glycerol carbonate to prevent the reversible reaction, which leads to difficulties in product separation making the entire process nonviable.<sup>[6,7]</sup>

The carbonylation of glycerol using urea as a carbonating agent overcomes the practical difficulties observed earlier. Urea is an inexpensive raw material produced by the reaction of carbon dioxide and ammonia by Bosch–Meiser urea process. Moreover, ammonia, the byproduct in glycerol carbonylation reaction can be utilized for the synthesis of urea by further reacting with carbon dioxide which in turn leads to an atom-efficient and greener process.

Glycerol carbonylation reaction using urea has been studied with different heterogeneous catalysts such as ZnO, HTc–Zn derived from hydrotalcite, Sn–Beta,<sup>[8]</sup> γ-zirconium phosphate,<sup>[9]</sup>

[a] P. Manjunathan, Dr. G. V. Shanbhag  
Materials Science Division, Poornaprajna Institute of Scientific Research  
Bidalur Post, Devanahalli, Bangalore-562164, Karnataka (India)  
E-mail: shanbhag@poornaprajna.org

[b] Dr. R. Ravishankar  
Hindustan Petroleum Green Research and Development Centre  
Hindustan Petroleum Corporation Ltd. (HPCL)  
KIADB Industrial Area, Tarabahalli, Hoskote Taluk  
Bangalore-560067, Karnataka (India)

Supporting Information for this article is available on the WWW under  
<http://dx.doi.org/10.1002/cctc.201501088>.

Sn–W mixed metal oxides,<sup>[10]</sup> La<sub>2</sub>O<sub>3</sub>,<sup>[11]</sup> Co<sub>3</sub>O<sub>4</sub>/ZnO,<sup>[12]</sup> Au/Fe<sub>2</sub>O<sub>3</sub>,<sup>[13]</sup> Sm<sub>0.6</sub>TPA,<sup>[14]</sup> Zn<sub>1</sub>TPA,<sup>[15]</sup> ZnSn(OH)<sub>6</sub>,<sup>[16]</sup> Zn-exchanged zeolites,<sup>[17]</sup> Zn/MCM-41,<sup>[18]</sup> and quaternary ammonium ion exchanged montmorillonite.<sup>[19]</sup> Among them, the zinc based catalysts have shown a promising activity because of their Lewis acidic nature. Notably, the catalyst with a combination of Lewis acid and base sites showed better performance yielding high amount of glycerol carbonate.

Binary or mixed metal oxides are widely used in industry as well as in academia which constitute the largest family of heterogeneous catalysts for the selective organic transformation reactions. Binary metal oxides are oxygen-containing compounds formed by the combination of two metal cations that may either vary or be defined by a strict stoichiometry. Owing to the presence of  $M^{n+}O^{m-}$  ion pairs in metal oxide, it is found to exhibit acid–base and redox properties. The extent of basicity depends on the coordination number of oxygen species present in the metal oxides. The metal ions in multimetallic oxides differ in their coordination environment that governs the type of bonding between the cations resulting in synergistic effect. For example; the two different metal cations can be represented as  $M_A^{n+}$  and  $M_B^{m+}$  in polyhedra, which connect in various possible ways such as edge- or corner-sharing  $M_A-O-M_B-O$ ,  $M_A-O-M_A-O$  or  $M_B-O-M_B-O$  metal–oxygen chains. This gives different cation environments leading to different active centers and different reactivity towards an approaching molecule.<sup>[18,20–22]</sup>

Herein, we report the bifunctional Zn–Sn composite oxide catalyst for the eco-friendly synthesis of glycerol carbonate from glycerol with urea. The influence of catalyst preparation methods towards its catalytic activity was systematically studied by three different routes, namely, coprecipitation, solid-state and evaporation methods. A series of active Zn–Sn composite oxide catalysts were prepared with varying Zn-to-Sn molar ratio. Further, the most active Zn–Sn composite oxide was treated at different temperatures to vary its catalytic properties. Two decisive catalyst properties, namely, acidity and basicity of the active catalyst were correlated with catalytic activity. The effect of reaction parameters on catalytic activity such as catalyst concentration, reaction temperature, and reaction time was also studied.

## Results and Discussion

The XRD patterns of Zn–Sn composite oxides prepared by using three different methods are shown in Figure 1 and Supporting Information, Figure S.1.1a. Zn–Sn composite oxide prepared through solid-state (SS) and evaporation method (Evp), respectively, showed a main phase of ZnO and SnO<sub>2</sub> along with a little spinel crystalline phase of Zn<sub>2</sub>SnO<sub>4</sub>. Conversely, Zn–Sn composite oxide prepared by coprecipitation method (CoPre) showed the main diffraction peak of spinel structured Zn<sub>2</sub>SnO<sub>4</sub> with the co-existence of ZnO and SnO<sub>2</sub>. The reason for the formation of Zn<sub>2</sub>SnO<sub>4</sub> as the major component can be explained as follows. The coprecipitation of Zn and Sn salts results in mainly a perovskite-type Zn–Sn hydroxide as the intermediate before the calcination step.<sup>[16]</sup> Upon calcination to

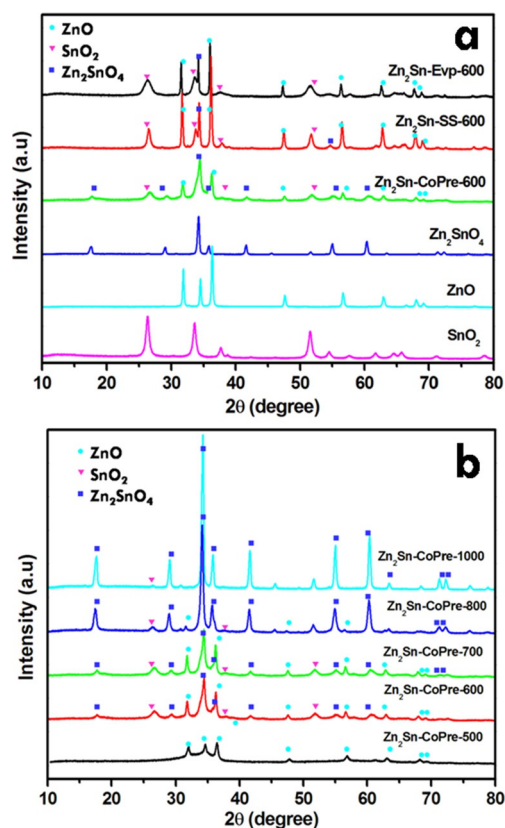


**Figure 1.** XRD patterns of (a) individual and composite Zn–Sn oxides prepared by three different methods with Zn/Sn = 2, (b) Zn<sub>2</sub>Sn–CoPre catalysts prepared at different calcinations temperatures.

600 °C, Zn–Sn hydroxide undergoes dehydroxylation leading to the formation of Zn<sub>2</sub>SnO<sub>4</sub> spinel.

The XRD patterns of the Zn-rich Zn–Sn composite oxides prepared with coprecipitation method clearly showed the increase of wurtzite-structured ZnO with increasing of Zn/Sn molar ratio in the range of 1–3 as shown in the Supporting Information, Figure S.1.1.b. The result indicates that the catalysts exhibit the combination of Zn<sub>2</sub>SnO<sub>4</sub> spinel, ZnO, and SnO<sub>2</sub> phases.

The XRD patterns of Zn<sub>2</sub>Sn–CoPre catalyst calcined at different temperatures are shown in Figure 1 b. It can be seen that the calcination temperature has a significant role in the formation of different phases. Zn<sub>2</sub>Sn–CoPre catalyst showed a gradual increase in crystallinity with increasing calcination temperature in the range of 500–1000 °C. The catalyst Zn<sub>2</sub>Sn–CoPre calcined at 500 °C showed the existence of only ZnO phase with lower intensity suggesting the presence of tin oxide in the amorphous state. However, at calcination temperatures of 600 and 700 °C, phases corresponding to Zn<sub>2</sub>SnO<sub>4</sub> spinel were formed with ZnO and SnO<sub>2</sub> in minor quantities. Further, ZnO phase disappeared above 800 °C giving rise to Zn<sub>2</sub>SnO<sub>4</sub> spinel and SnO<sub>2</sub> phases.

The textural properties of Zn–Sn composite oxide catalysts are tabulated in Table 1. The catalysts prepared through the evaporation method showed larger surface area and pore volume than those prepared by the other two routes. The Zn–

**Table 1.** Physico-chemical properties of individual and Zn–Sn composite oxides.

Catalyst	Calcination temp. [°C]	$S_{\text{BET}}^{[a]}$ [ $\text{m}^2 \text{g}^{-1}$ ]	Pore volume <sup>[b]</sup> [ $\text{cm}^3 \text{g}^{-1}$ ]	Pore size <sup>[c]</sup> [nm]	Acidity [ $\mu\text{mol}_{\text{NH}_3} \text{g}^{-1}$ ] <sup>[d]</sup>	Basicity [ $\mu\text{mol}_{\text{CO}_2} \text{g}^{-1}$ ] <sup>[e]</sup>
ZnO	600	18.9	0.022	4.6	60	12
SnO <sub>2</sub>	600	16.6	0.066	15.8	30	4
Zn <sub>2</sub> SnO <sub>4</sub>	600	40.0	0.150	3.7	160	20
Zn <sub>1</sub> Sn–CoPre	600	13.3	0.056	17.0	235	52
Zn <sub>2</sub> Sn–CoPre	600	15.2	0.049	12.6	268	61
Zn <sub>3</sub> Sn–CoPre	600	17.0	0.046	10.9	256	48
Zn <sub>1</sub> Sn–SS	600	8.9	0.055	24.7	216	38
Zn <sub>2</sub> Sn–SS	600	9.2	0.050	22.7	223	45
Zn <sub>1</sub> Sn–Evp	600	31.5	0.132	16.7	181	35
Zn <sub>2</sub> Sn–Evp	600	33.2	0.130	16.5	210	48
Zn <sub>2</sub> Sn–CoPre	500	25.0	0.052	8.4	207	30
Zn <sub>2</sub> Sn–CoPre	600	15.2	0.049	12.6	268	61
Zn <sub>2</sub> Sn–CoPre	700	14.1	0.047	13.2	240	53
Zn <sub>2</sub> Sn–CoPre	800	6.0	0.024	16.3	155	27
Zn <sub>2</sub> Sn–CoPre	1000	3.0	0.007	9.3	100	7

[a] BET surface area, [b] Total pore volume, [c] Average pore diameter, [d] NH<sub>3</sub>TPD, [e] CO<sub>2</sub>TPD.

Sn composite oxides prepared by coprecipitation and solid-state routes gave lower surface area than ZnO, whereas the pore volume was in between that of ZnO and SnO<sub>2</sub>. However, a marginal increase in surface area was observed upon increasing the Zn content in Zn/Sn composition for the three catalyst preparation methods. The effect of calcination on Zn<sub>2</sub>Sn–CoPre catalysts showed that with increasing calcinations temperature, the surface area and pore volume decline because of the agglomeration of particles.

The amount of acidity in Zn–Sn composite oxide catalysts was determined by temperature-programmed desorption (TPD) technique using ammonia as a probe molecule as tabulated in Table 1. Zn–Sn composite oxide prepared through coprecipitation method contained a higher amount of acidity than the composite oxides prepared by other preparation methods. The total acidity of catalysts prepared by different methods decreased in the order: coprecipitation > solid state > evaporation.

A gradual increase in total acidity was observed with the increase in Zn/Sn molar ratio from 1 to 2. Amongst the catalysts, Zn<sub>2</sub>Sn–CoPre-600 showed the highest amount of acidity. In contrast, further increase in Zn/Sn molar ratio to 3 gave a marginal decrease of acidity.

The presence of basic sites in Zn–Sn composite oxides was investigated by CO<sub>2</sub>TPD and the amount of basicity is represented in Table 1. Basically, the lattice oxygens present on the metal oxide surface are considered to act as Lewis basic sites.<sup>[22]</sup> As observed for NH<sub>3</sub> TPD, Zn–Sn composite oxides also showed an increase of basic sites with increase in Zn/Sn molar ratio from 1 to 2, however, further increase of Zn/Sn to 3 resulted in the decrease of total basicity. The Zn<sub>2</sub>Sn–CoPre catalysts exhibited a greater amount of basic sites than the catalysts prepared by other methods, and Zn<sub>2</sub>Sn–CoPre-600 showed highest amount of basicity.

The results from NH<sub>3</sub> and CO<sub>2</sub> TPD of Zn<sub>2</sub>Sn–CoPre catalysts obtained from different calcination temperatures exhibited interesting results (Table 1). The increase in calcination tempera-

ture from 500–600 °C results in an increase of total active sites (acidity and basicity) owing to the formation of mixed phase as observed in XRD pattern. However, a further increase in calcination temperature above 600 °C leads to a decrease in the amount of total active sites (acidity and basicity). This could be attributed to the decreased amount of metal–oxygen pairs on the surface caused by the decrease of surface area in Zn–Sn composite oxide.<sup>[22]</sup> As a result, Zn<sub>2</sub>Sn–CoPre-600 catalyst possesses a relatively higher amount of total active sites than other samples.

SEM analysis of Zn–Sn composite oxide catalysts revealed the particle size and morphology as shown in Figure 2. Depending on the adopted catalyst preparation methods, the morphology and particle sizes varied. Amongst them, Zn<sub>1</sub>Sn–Evp-600 showed larger particle sizes ranging between 2 and 30 μm (average of 8.3 μm), possessing nonuniform particles with rough edge surface. Irregular morphology of uniformly dispersed ZnO on the SnO<sub>2</sub> surface was observed with Zn<sub>1</sub>Sn–SS-600. And the particle size was in the range of 0.4–1.6 μm. In the case of Zn<sub>1</sub>Sn–CoPre-600, the particle size was in the range of 0.5–4 μm with octahedral morphology containing an average particle size of 1.6 μm.

The change in Zn/Sn mole ratio prepared by the coprecipitation method resulted in a different morphology with varying particle size (Figure 2c, d, f). Zn<sub>2</sub>Sn–CoPre-600 possessed cubic shape with the particle size ranging from 0.8 to 2.5 μm and the average particle size was 1.6 μm. Zn<sub>3</sub>Sn–CoPre-600 exhibited octahedral morphology with particle sizes in the range of 0.9–2.5 μm (average size = 1.7 μm).

Interestingly, SEM images of Zn<sub>x</sub>Sn–CoPre-600 (x = 1–3) showed some protuberance on the surface of octahedral or cubic morphology. It could be caused by the growth of ZnO by the secondary nucleation from the excess of Zn species. As the Zn/Sn molar ratio increases from 2 to 3, the formation of ZnO from secondary nucleation masks the octahedral surface. Moreover, the particle size of ZnO formed on the cubic or octahedral surface lies in the nano regime (< 100 nm) and it is

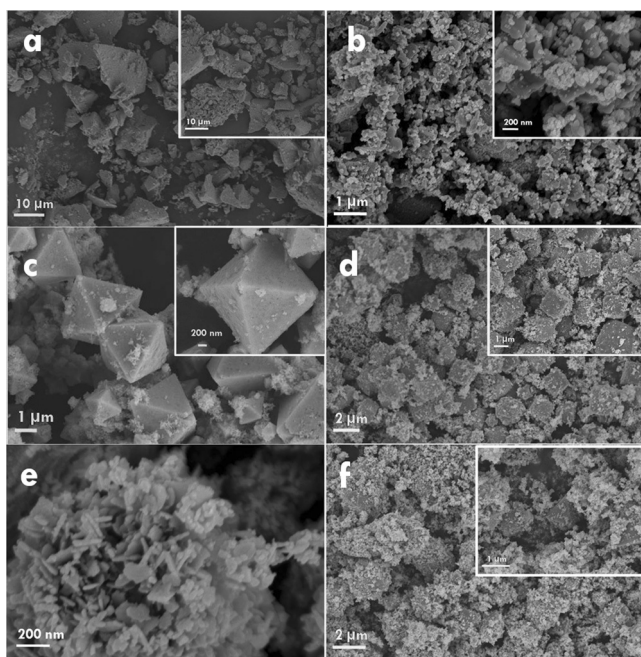


**Figure 2.** SEM images of (a) Zn<sub>1</sub>Sn-Evp-600, (b) Zn<sub>1</sub>Sn-SS-600, (c) Zn<sub>1</sub>Sn-CoPre-600, (d) Zn<sub>2</sub>Sn-CoPre-600, (e) Zn<sub>2</sub>Sn-CoPre-600 (secondary nucleation on cubic surface), and (f) Zn<sub>2</sub>Sn-CoPre-600.

composed of weakly agglomerated small-flake-like particles. (Figure 2 e).

TEM images of Zn<sub>2</sub>Sn-CoPre-600 are shown in Figure 3 a–f. The TEM images in Figure 3 a and 3 b show cubic morphology with the size ranging from 0.5 to 2 μm along with other particles in the nanosized range. The corresponding high-resolution (HR) TEM micrograph of the cubic morphology is shown in Figure 3 c, which reveals well-defined lattice fringes with *d*-spacings of 0.33 and 0.28 nm corresponding to (220) and (311) planes of Zn<sub>2</sub>SnO<sub>4</sub>, respectively.<sup>[23]</sup> In Figure 3 d, the TEM image of nanoparticles grown near the cubic morphology is shown. The HRTEM image of the nanoparticles shows the *d*-spacing of 0.33 and 0.28 nm corresponding to (110) and (100) planes of SnO<sub>2</sub> and ZnO, respectively, confirming the presence of nanocrystalline particles of the SnO<sub>2</sub> and ZnO.

## Catalytic activity studies

### Performance of Zn–Sn composite metal oxide catalyst

The catalytic behavior of Zn<sub>1</sub>Sn composite oxides prepared through different routes was evaluated for the carbonylation reaction of glycerol with urea and the results are tabulated in Table 2. The reaction without catalyst resulted in only 32% of glycerol conversion with 95% glycerol carbonate selectivity. Pure oxides of Zn and Sn, and bimetallic oxides of Zn and Sn were individually tested as catalysts. These oxides showed moderate activity of 66.4% (ZnO), 39.6% (SnO<sub>2</sub>), and 50% (Zn<sub>2</sub>SnO<sub>4</sub>) glycerol conversion with glycerol carbonate selectivity of 98, 99 and 96% respectively. The other minor products formed during the reaction were glycerol carbamate, glycidol,

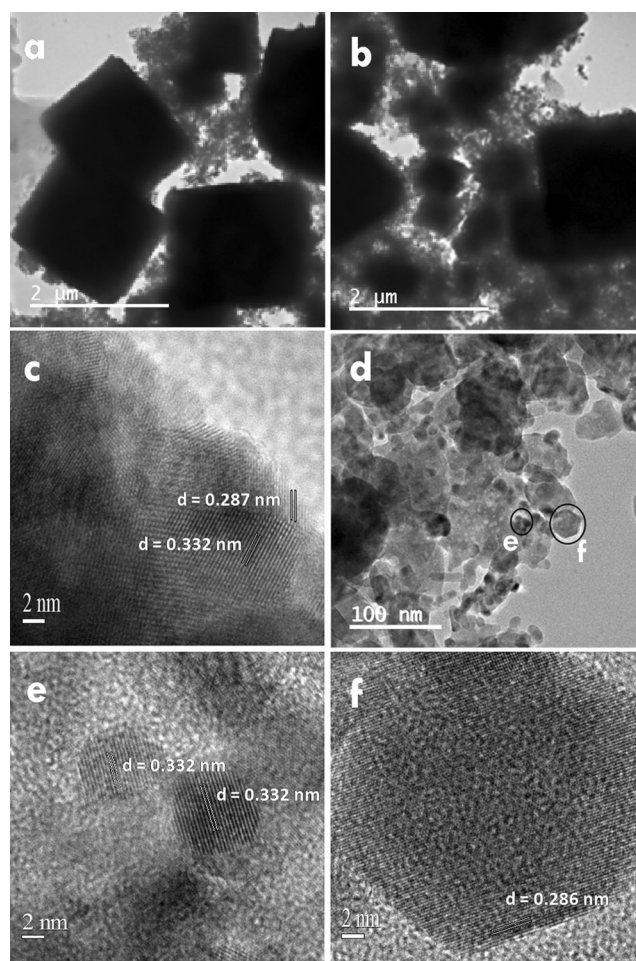


**Figure 3.** TEM and HRTEM images of Zn<sub>2</sub>Sn-CoPre-600: (a) and (b) TEM image; (c) HRTEM image of cubic particles; (d) TEM image of secondary particles; (e) HRTEM image of the small circled area in (d); (f) HRTEM image of the large circled area in (d).

**Table 2.** Total active sites and activities of different catalysts for glycerol carbonylation reaction.<sup>[a]</sup>

Catalyst	Total active sites [μmol g <sup>-1</sup> ] <sup>[b]</sup>	Glycerol conversion [wt%]	GlyC selectivity [wt%]	GlyC yield [wt%]
blank	–	32.0	95.8	30.6
ZnO	72	66.4	98.1	65.1
SnO <sub>2</sub>	34	39.6	99.0	39.2
Zn <sub>2</sub> SnO <sub>4</sub>	180	50.0	96.0	48.0
Zn <sub>1</sub> Sn-CoPre-600	287	88.0	99.2	87.3
Zn <sub>1</sub> Sn-SS-600	254	79.5	99.4	79.0
Zn <sub>1</sub> Sn-Evp-600	216	76.1	99.2	75.5

[a] Reaction conditions: glycerol = 2 g, urea = 1.31 g, catalyst = 0.33 g, temperature = 155 °C, time = 4 h, under N<sub>2</sub> bubbling, [b] from TPD analysis (sum of acidity and basicity). GlyC = glycerol carbonate.

(2-oxo-1,3-dioxolan-4-yl)methylcarbamate, and 5-(hydroxymethyl)-1,3-oxazolidin-2-one.

The Zn–Sn composite oxides exhibited higher catalytic activity than the individual oxides. Among the composite oxides, higher activity depended on the specific catalyst preparation

procedure adopted.  $Zn_1Sn$ -CoPre-600 catalyst gave 88% of glycerol conversion with approximately 99% selectivity for glycerol carbonate. In addition,  $Zn_1Sn$ -SS-600 and  $Zn_1Sn$ -Evp-600 gave 79.5% and 76%, respectively, with 99.2% glycerol carbonate selectivity. Amongst the Zn–Sn composite oxides,  $Zn_1Sn$ -CoPre-600 gave the best performance considering the glycerol carbonate yield. The superior catalytic activity is mainly attributed to the presence of higher amount of active sites (see Table 2). The lower activities of ZnO,  $SnO_2$ , and  $Zn_2SnO_4$  compared to that of the composite oxides are mainly caused by the lower amount of active sites present in the catalyst. As a correlation, an enhanced catalytic activity in  $Zn_1Sn$  composite oxide catalyst was observed with the increase of both acidic and basic site. The yield of glycerol carbonate over  $Zn_1Sn$  catalysts prepared through different routes decreased with decrease in the amount of active sites in the following trend:  $Zn_1Sn$ -CoPre-600 >  $Zn_1Sn$ -SS-600 >  $Zn_1Sn$ -Evp-600.

### Effect of Zn content in Zn–Sn composite oxides

The Zn–Sn composite oxides prepared through coprecipitation method exhibited high catalytic activity for glycerol carbonate synthesis. Therefore, the effect of Zn/Sn molar ratio on the catalytic activity was investigated from Zn/Sn = 1 to 3. The increase of Zn content in Zn–Sn composite oxide resulted in a substantial improvement in glycerol conversion from 88% ( $Zn_1Sn$ -CoPre-600) to 96% ( $Zn_2Sn$ -CoPre-600) with  $\geq 99\%$  selectivity for glycerol carbonate as shown in Table 3. Further in-

Catalyst	Total active sites [ $\mu\text{mol g}^{-1}$ ] <sup>[b]</sup>	Glycerol conversion [wt %]	GlyC selectivity [wt %]	GlyC yield [wt %]
$Zn_1Sn$ -CoPre-600	287	88.0	99.2	87.3
$Zn_2Sn$ -CoPre-600	329	96.0	99.6	95.6
$Zn_3Sn$ -CoPre-600	304	90.7	98.7	89.5
$Zn_2Sn$ -SS-600	268	84.0	99.2	83.3
$Zn_2Sn$ -Evp-600	258	80.0	99.0	79.2

[a] Reaction conditions: Glycerol = 2 g, urea = 1.31 g, catalyst = 0.33 g, temperature = 155 °C, time = 4 h, under  $N_2$  bubbling, [b] From TPD analysis (sum of acidity and basicity). GlyC = glycerol carbonate.

crease of Zn content from 2 to 3 ( $Zn_3Sn$ -CoPre-600) resulted in a marginal decrease of glycerol conversion by approximately 5% and a minor decrease in glycerol carbonate selectivity. The enhanced catalytic activity of  $Zn_2Sn$ -CoPre-600 catalyst could be the result of the presence of higher amount of active sites than for other catalysts.

The catalysts prepared by the other two methods with best composition of Zn/Sn = 2 were also evaluated for the synthesis of glycerol carbonate and compared with  $Zn_2Sn$ -CoPre-600 prepared by coprecipitation. These catalysts,  $Zn_2Sn$ -SS-600 and  $Zn_2Sn$ -Evp-600, showed lower catalytic activity (84 and 80% conversion, respectively) than  $Zn_2Sn$ -CoPre-600 owing to the presence of lower amount of active sites.

### Effect of the calcination temperature of most active $Zn_2Sn$ -CoPre catalyst on the catalytic activity

It is well known that the calcination temperature of metal oxides has an influence on composition, surface area, and active sites of the catalyst. Therefore, the effect of calcination temperature of  $Zn_2Sn$ -CoPre was studied by varying the calcination temperature ranging from 500 to 1000 °C. The catalytic activity of the calcined catalysts was evaluated and the results are depicted in Figure 4. The glycerol conversion increased ap-

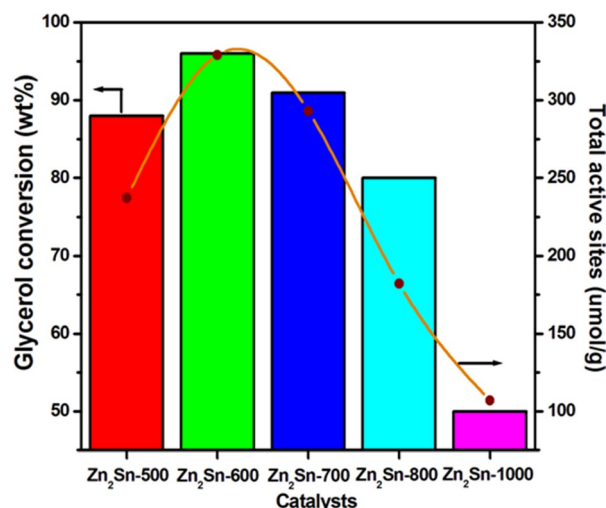


Figure 4. Effect of calcination temperature on catalytic activity. Reaction conditions: glycerol (2 g), urea (1.31 g), catalyst (0.33 g),  $T = 155$  °C,  $t = 4$  h, under  $N_2$  bubbling.

preciably from 88.5 to 96% upon increasing calcination temperature from 500 to 600 °C along with an increase in glycerol carbonate selectivity (98.5 to 99.6%). However, with further increasing calcination temperature from 600 to 1000 °C, the catalytic activity decreased considerably (glycerol conversion decreased from 96 to 50%). To understand the catalytic behavior of the catalysts calcined at different temperatures, the physicochemical properties and their relationship with catalytic performance were studied (see Table 1). It is found that the amount of total active sites decreased with increasing calcination temperature from 600 to 1000 °C, and  $Zn_2Sn$ -CoPre-600 possesses more total active sites than other catalysts. The decrease in active sites upon increase of calcination temperature could be attributed to the decrease of surface area owing to the agglomeration of particles resulting in less surface metal–oxygen pairs.<sup>[22]</sup> The relationship between total active sites of the catalyst and their catalytic activity towards glycerol conversion is depicted in Figure 4. The enhanced catalytic behavior of  $Zn_2Sn$ -CoPre-600 was mainly attributed to the presence of a higher amount of total active sites compared to other catalysts.

### Influence of the reaction conditions

The reaction temperature has a profound effect on the catalytic behavior. Therefore, a systematic study using  $Zn_2Sn$ -CoPre-600 catalyst was conducted from 145 to 175 °C with the glycer-

ol/urea mole ratio of 1:1 and 10 wt% of catalyst. Glycerol conversion increased significantly from 78.5 to 96% with an increase in temperature from 145 to 155 °C with a marginal increase of glycerol carbonate selectivity (98.7 to 99.6%) as shown in Figure 5a. Glycerol conversion and glycerol carbonate selectivity decreased marginally with further increase in reaction temperature from 165 to 175 °C. Therefore, 155 °C was the best reaction temperature and hence it was selected for further studies.

The effect of catalyst amount towards glycerol carbonate synthesis was studied by using Zn<sub>2</sub>Sn-CoPre-600 from 5 to 15 wt% of total reactant weight as shown in Figure 5b. As the catalyst amount increased from 5 to 10 wt%, the glycerol conversion increased significantly from 82 to 96% with an increase in glycerol carbonate selectivity (98.2 to 99.6%) attributed to the increase in the number of accessible active sites. The conversion remained almost the same with further increase in catalyst amount to 12.5 and 15 wt%. Hence, 10 wt% of catalyst loading is sufficient to yield high amount of glycerol carbonate and hence selected for further studies.

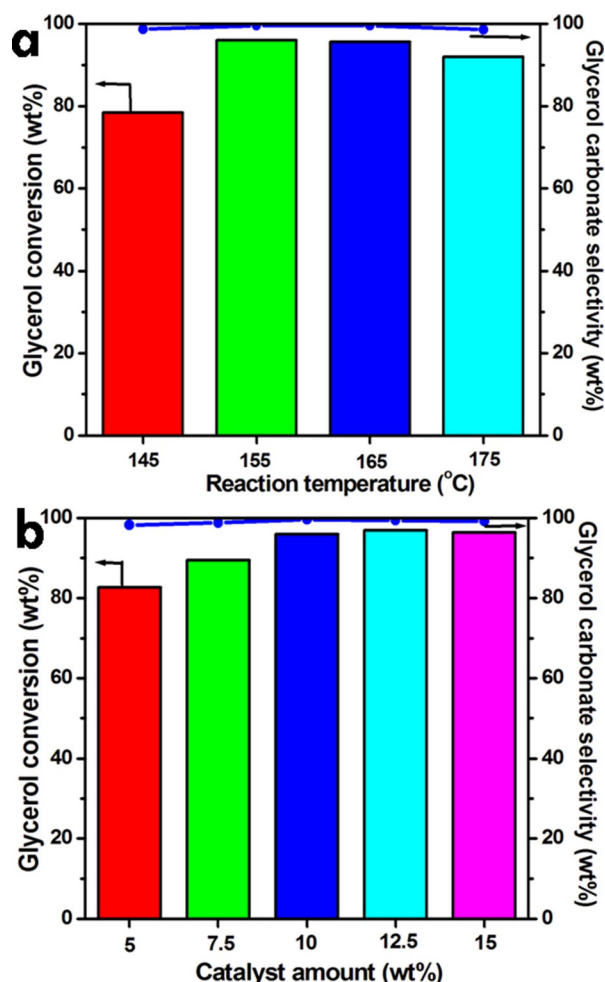


**Figure 5.** Influence of reaction conditions over glycerol carbonylation. (a) Effect of temperature: Reaction conditions: glycerol (2 g), urea (1.31 g), catalyst (0.33 g) Zn<sub>2</sub>Sn-CoPre-600, *t* = 4 h, under N<sub>2</sub> bubbling; (b) effect of catalyst amount: reaction conditions: glycerol (2 g), urea (1.31 g), catalyst Zn<sub>2</sub>Sn-CoPre-600, *T* = 155 °C, *t* = 4 h, under N<sub>2</sub> bubbling.

The effect of reaction time on the synthesis of glycerol carbonate was studied under the optimized reaction conditions. The results showed a significant increase in glycerol conversion with increase in reaction time as shown in the Supporting Information, Figure S.1.2. Initially it gave 50% conversion after 1 h, which further increased to 96% after 4 h with a marginal increase in glycerol carbonate selectivity (98 to 99.6%).

### Recycling studies

The most active Zn<sub>2</sub>Sn-CoPre-600 catalyst was studied for its reusability and the results are presented in Figure 6a. The Zn<sub>2</sub>Sn-CoPre-600 catalyst was tested under optimized reaction conditions for five consecutive runs (Fresh, R-1, R-2, R-3, and R-4). After each run, the catalyst was filtered and washed with methanol to remove the adsorbed reactants on the catalyst surface. The catalyst was dried and finally calcined at 600 °C for 4 h. Zn<sub>2</sub>Sn-CoPre-600 catalyst showed good recyclability with marginal decrease in the activity as shown in Figure 6a. The yield for glycerol carbonate was 95.6% after the first cycle and it decreased marginally to 90.6% after 5 cycles. These results suggest that the Zn<sub>2</sub>Sn-CoPre-600 catalyst is stable and reusable without any appreciable loss in activity. The structural integrity of the recycled catalyst was examined by X-ray diffraction as shown in Figure 6b. The XRD pattern of the spent Zn<sub>2</sub>Sn-CoPre-600 catalyst matched well with the characteristic peaks of fresh catalyst indicating no change in the structure of the catalyst even after five consecutive cycles.

To determine the leached zinc species during the reaction, atomic absorption spectroscopy (AAS) was performed. After the completion of reaction, the reaction medium was filtered and the filtrate was subjected to AAS. It showed a small amount of zinc dissolved ( $\approx 1\%$ ) in the reaction mixture attributed to the formation of zinc glycerolate, which is commonly observed for ZnO-containing catalysts.<sup>[22]</sup>

### Comparison of Zn–Sn composite oxide with reported solid acid catalysts

The catalytic performance of Zn–Sn composite oxide was compared with that of other solid catalysts reported in the literature as shown in Table 4. The acid catalysts namely Sn-beta,<sup>[8]</sup> Au/Fe<sub>2</sub>O<sub>3</sub>,<sup>[3]</sup> and Sm<sub>0.66</sub>TPA<sup>[14]</sup> showed high glycerol conversion with lower glycerol carbonate selectivity and vice versa observed with Zn<sub>1</sub>TPA,<sup>[15]</sup> 2.5% Au/Nb<sub>2</sub>O<sub>5</sub>,<sup>[13]</sup> and Sn–W mixed oxide.<sup>[8]</sup> The catalysts containing acid–base property, specifically zirconium phosphate<sup>[9]</sup> and ZnSn(OH)<sub>6</sub>,<sup>[16]</sup> exhibited approximately 100% glycerol carbonate selectivity with high glycerol conversion. The zinc-exchanged HY zeolite<sup>[17]</sup> showed 94.6% glycerol conversion with 98% selectivity to glycerol carbonate. The performance of Zn–Sn composite oxide catalyst (Zn<sub>2</sub>Sn-CoPre-600) in the present study was at par with the best of the reported catalysts.

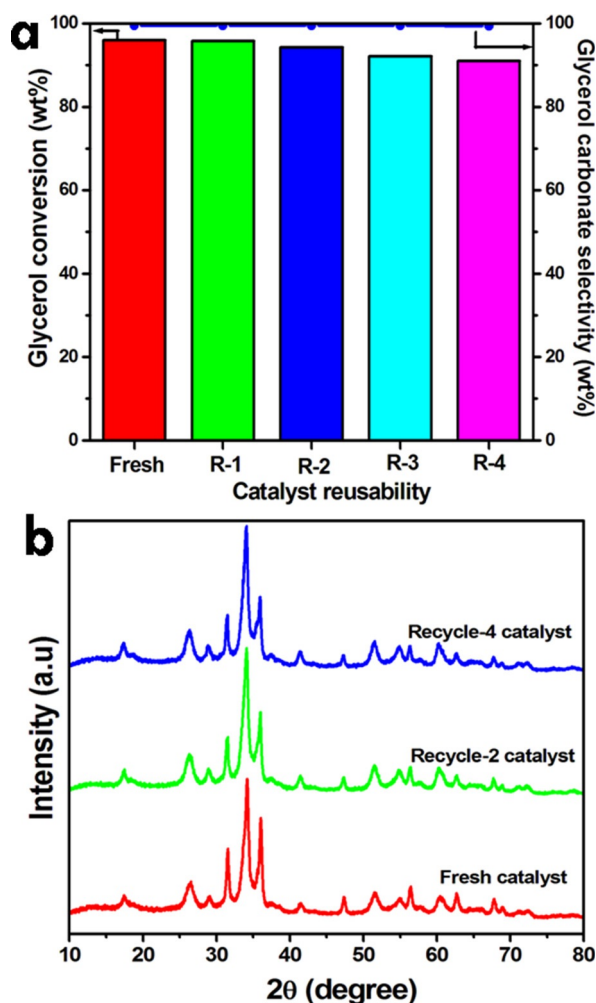


**Figure 6.** (a) Recycling of  $Zn_2Sn$ -CoPre-600 catalyst for the carbonylation reaction. Reaction conditions: glycerol (4 g), urea (2.62 g), catalyst amount = 0.66 g,  $T = 155^\circ C$ , time = 4 h, under  $N_2$  bubbling. (b) XRD patterns of recycled catalyst ( $Zn_2Sn$ -CoPre-600).

### Reaction mechanism

It was found that the synthesis of cyclic carbonates from alcohol and urea is catalyzed by the combination of Lewis acid and Lewis base sites present in the catalyst. Based on the

above findings, a plausible reaction mechanism is proposed for  $Zn$ - $Sn$  composite oxide catalyzed carbonylation of glycerol with urea and shown in Scheme 1. In the first step, the basic sites present in  $Zn$ - $Sn$  catalyst activate the hydroxyl group of glycerol, whereas the Lewis acidic  $Zn$  activates the carbonyl group of urea. In the second step, the lone pair of electron present on the hydroxyl group of glycerol attacks the carbonyl carbon and forms an intermediate with the elimination of ammonia. In the last step, this intermediate undergoes cyclization by the attack of adjacent hydroxyl group on the tertiary carbocation leading to the formation of glycerol carbonate with the elimination of another molecule of ammonia.

### Conclusions

Zinc-Tin composite oxide catalysts were synthesized by three different methods and evaluated for the synthesis of glycerol carbonate by carbonylation of glycerol with urea. The composite oxide contained three components, namely,  $Zn_2SnO_4$ ,  $ZnO$ , and  $SnO_2$ . These catalysts showed high activity towards the selective synthesis of glycerol carbonate compared to individual oxides.  $Zn$ - $Sn$  composite oxide catalyst prepared from coprecipitation showed excellent catalytic performance compared to the catalysts prepared by other methods. The superior catalytic activity of the  $Zn$ - $Sn$  composite catalyst prepared by coprecipitation method ( $ZnSn$ -CoPre) is mainly attributed to the presence of high amounts of acidic and basic sites. The activity of  $Zn$ - $Sn$  composite oxide catalysts depends upon the  $Zn/Sn$  mole ratio as well as calcination temperature. The better catalytic activity was obtained over the catalyst with the  $Zn/Sn$  mole ratio of 2 calcined at  $600^\circ C$ . A good correlation between the catalytic activity and the amount of active sites was observed. Thus, bifunctional  $Zn_2Sn$ -CoPre-600 catalyst is shown to be the novel and highly efficient catalyst for carbonylation of glycerol with urea.

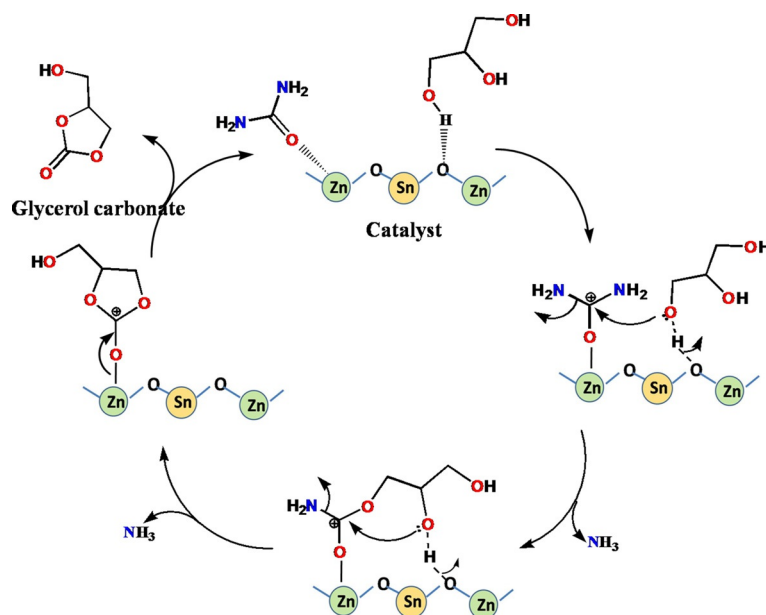
## Experimental Section

### Catalyst preparation

Preparation of  $Zn$ - $Sn$  composite oxides, method A (coprecipitation route): In a typical procedure for  $Zn/Sn$  molar ratio of 2, anhydrous

**Table 4.** Comparison of  $Zn$ - $Sn$  composite oxide with reported solid acid catalysts.

Catalyst	$T$ [ $^\circ C$ ]	Reaction time [h]	Glycerol conv. [%]	Glycerolcarbonate [%]		Ref.
				Selectivity	Yield	
SW21	140	4	52.1	95.3	49.7	[10]
Sn-beta	145	5	70.0	37.0	25.9	[8]
Zr-P	140	3	80.0	100	80.0	[9]
Au/ $Fe_2O_3$	150	4	80.0	48.0	38.4	[13]
2.5% Au/ $Nb_2O_5$	150	4	66.0	32.0	21.1	[13]
$Sm_{0.66}$ TPA	140	4	49.5	85.4	42.3	[14]
$Zn_1$ TPA	140	4	69.2	99.4	68.8	[15]
$ZnSn(OH)_6$	165	5	98.0	99.6	97.6	[16]
$La_2O_3$	140	4	68.9	98.1	67.6	[11]
$Zn_2Sn$ -CoPre-600	155	4	96.0	99.6	95.6	this work



**Scheme 1.** Plausible reaction mechanism for the synthesis of glycerol carbonate over Zn–Sn catalyst.

ZnCl<sub>2</sub> (6.81 g, 1 M) and SnCl<sub>4</sub>·5H<sub>2</sub>O (8.76 g, 0.5 M) were dissolved in 50 mL of deionized water followed by dropwise addition of 83 mL of 4 M NaOH solution. The precipitate was stirred for 3 h at RT, filtered, washed with deionized water until it was free from chloride and dried at 120 °C overnight. The dried catalyst was subjected to calcination at 5 °C min<sup>-1</sup> for 4 h under static air and designated as Zn<sub>x</sub>Sn-*y*-*z* (*x* = zinc to tin mole ratio, *y* = synthesis route, *z* = calcination temperature in °C). The above sample was thus designated as Zn<sub>2</sub>Sn-CoPre-*z*.

Zn–Sn composite oxide with different Zn/Sn molar ratios (Zn/Sn = 1, and 3) were prepared by changing the molar ratios of the starting metal salt solutions and sodium hydroxide concentration. The hydroxides obtained were subjected to calcination at 600 °C for 4 h under static air. The catalysts are denoted as Zn<sub>1</sub>Sn-CoPre-600 and Zn<sub>3</sub>Sn-CoPre-600.

**Preparation of Zn–Sn composite oxides, method B (solid-state route):** The mechanical mixtures of ZnO and SnO<sub>2</sub> with molar ratios of 1:1 and 2:1 were prepared as follows. In a typical procedure, ZnO and SnO<sub>2</sub> powders were taken with a required Zn/Sn molar ratio (= 1 or 2) and they were mechanically ground by using mortar and pestle for 30 min. Finally, the sample was subjected to calcination at 600 °C for 4 h at 5 °C min<sup>-1</sup> under static air. The sample was designated as Zn<sub>x</sub>Sn-SS-600 (where *x* = 1 or 2).

**Preparation of Zn–Sn composite oxides, method C (evaporation route):** Zinc chloride and tin chloride salts with required mole ratio of Zn/Sn (= 1 or 2) were dissolved in distilled water and allowed to evaporate to complete dryness. Later, the dried sample was subjected to calcination at 600 °C for 4 h and the obtained sample was designated as Zn<sub>x</sub>Sn-Evp-600 (with *x* = 1 or 2).

**Preparation of pure oxides:** ZnO was prepared by precipitation route with the following procedure. 1 M NaOH solution (83 mL) was added dropwise to the beaker containing 50 mL of 0.5 M aqueous ZnCl<sub>2</sub> solution. The obtained precipitate was allowed to stir for 3 h, filtered, washed, and dried at 120 °C overnight. The dried product was ground into fine powder and calcined at 600 °C for 4 h. SnO<sub>2</sub> was prepared with above-mentioned procedure with 2 M concentration of NaOH and 0.5 M aqueous SnCl<sub>4</sub>·5H<sub>2</sub>O.

**Preparation of Zn<sub>2</sub>SnO<sub>4</sub>:** Zn<sub>2</sub>SnO<sub>4</sub> was prepared from the reported literature<sup>[24]</sup> and calcined at 600 °C for 4 h.

### Catalyst characterization

Powder X-ray diffraction patterns of the catalysts were recorded with Bruker D2 phaser X-ray diffractometer using Cu<sub>Kα</sub> radiation ( $\lambda = 1.5418 \text{ \AA}$ ) with high resolution Lynxeye detector. All the samples were scanned in the  $2\theta$  range of 10–80° with step size of 0.04° s<sup>-1</sup>. The specific surface area, pore volume and pore size of the catalysts were determined from nitrogen sorption measurement using Quantachrome NOVA instrument at 77 K. The amount of acidity and basicity present in the catalysts were determined by TPD equipped with thermal conductivity detector (using NH<sub>3</sub> and CO<sub>2</sub>, respectively). In all the experiments, the sample (400 mg) was calcined at the desired temperature for 1 h in helium gas flow (25 mL min<sup>-1</sup>) and then cooled to 50 °C. At 50 °C, the sample was saturated with 10% of ammonia or carbon dioxide in a helium stream for 2 h. After the saturation of probe molecule, the sample was flushed with helium for 1 h at 50 °C to remove the physisorbed probe molecule, and then desorption of ammonia or carbon dioxide was performed in the temperature range from 50 to 600 °C with the heating rate of 8 °C min<sup>-1</sup>. SEM images of Zn–Sn composite oxide catalysts prepared by different methods were recorded on Zeiss microscope to investigate the particle size and morphology. TEM analyses were performed using TEM-JEOL-2010 instrument.

### Catalytic activity studies

The glycerol carbonylation reaction with urea was performed in a 50 mL 2-necked glass batch reactor equipped with a reflux condenser. In a typical experiment, the required amounts of glycerol (2 g) and urea (1.31 g) were taken along with preactivated catalyst (wt% referred to total reactant weight). The reaction mixture was magnetically stirred at required temperature with bubbling of nitrogen gas through the second neck of glass reactor to remove the evolved ammonia gas during the reaction. After the desired

time of reaction, the reaction mixture was dissolved in methanol and centrifuged to separate out the catalyst from the liquid phase. The obtained liquid was analyzed by gas chromatography (Agilent 7820A) equipped with a capillary column (0.25 mm I.D and 60 m length, HP-INNOWAX) and flame ionization detector. The products were confirmed by GCMS analysis. The glycerol conversion and glycerol carbonate selectivity were calculated using the following formulae:

Glycerol conversion (wt %)

$$= \frac{\text{wt of glycerol taken} - \text{wt of unreacted glycerol}}{\text{wt of glycerol taken}} \times 100$$

Product yield (wt %)

$$= \frac{\text{glycerol converted (wt\%)} \times \text{product selectivity}}{100}$$

## Acknowledgements

GVS is thankful to Vision Group on Science and Technology, Govt. of Karnataka, India for Centre of Excellence in Science Engineering and Medicine (CESEM) Grant (GRD No 307). PM acknowledges Admar Mutt Education Foundation (AMEF), Bangalore for providing a scholarship and thankful to Manipal University for permitting this research as a part of the Ph.D. program. Authors are thankful to CeNSE, Indian Institute of Science, Bangalore for SEM analysis.

**Keywords:** biomass · carbonylation · green chemistry · tin · zinc

- [1] C. Serrano-Ruiz, R. Luque, A. S. Escibano, *Chem. Soc. Rev.* **2011**, *40*, 5266–5281.  
[2] A. Behr, J. Eilting, K. Irawadi, J. Leschinsk, F. Linder, *Green Chem.* **2008**, *10*, 13–30.

- [3] B. Zhang, G. Ding, H. Zheng, Y. Zhu, *Appl. Catal. B* **2014**, *152–153*, 226–232.  
[4] M. J. Climent, A. Corma, S. Iborra, *Green Chem.* **2014**, *16*, 516–547.  
[5] P. Manjunathan, S. P. Maradur, A. B. Halgeri, G. V. Shanbhag, *J. Mol. Catal. A* **2015**, *396*, 47–54.  
[6] M. O. Sonnati, S. Amigoni, E. P. T. de Givenchy, T. Darmanin, O. Choulet, F. Guittard, *Green Chem.* **2013**, *15*, 283–306.  
[7] J. R. Ochoa-Gómez, O. G. J. Aberasturi, C. R. Lopez, M. Belsue, *Org. Process Res. Dev.* **2012**, *16*, 389–399.  
[8] M. J. Climent, A. Corma, P. D. Frutos, S. Iborra, M. Noy, A. Velty, P. Concepcion, *J. Catal.* **2010**, *269*, 140–149.  
[9] M. Aresta, A. Dibenedetto, F. Nocito, C. Ferragina, *J. Catal.* **2009**, *268*, 106–114.  
[10] K. Jagadeeswaraiyah, Ch. R. Kumar, P. S. S. Prasad, S. Loidant, N. Lingaiah, *Appl. Catal. A* **2014**, *469*, 165–172.  
[11] L. Wang, Y. Ma, Y. Wang, S. Liu, Y. Deng, *Catal. Commun.* **2011**, *12*, 1458–1462.  
[12] F. Rubio-Marcos, V. C. Casilda, M. A. Banares, J. F. Fernandez, *ChemCatChem* **2013**, *5*, 1431–1440.  
[13] C. Hammond, J. A. L. Sanchez, M. H. A. Rahim, N. Dimitratos, R. L. Jenkins, A. F. Carley, Q. He, C. J. Kiely, D. W. Knight, G. J. Hutchings, *Dalton Trans.* **2011**, *40*, 3927–3937.  
[14] Ch. R. Kumar, K. Jagadeeswaraiyah, P. S. S. Prasad, N. Lingaiah, *ChemCatChem* **2012**, *4*, 1360–1367.  
[15] K. Jagadeeswaraiyah, Ch. R. Kumar, P. S. S. Prasad, N. Lingaiah, *Catal. Sci. Technol.* **2014**, *4*, 2969–2977.  
[16] S. Sandesh, G. V. Shanbhag, A. B. Halgeri, *RSC Adv.* **2014**, *4*, 974–977.  
[17] V. S. Marakatti, A. B. Halgeri, *RSC Adv.* **2015**, *5*, 14286–14293.  
[18] S. E. Kondawar, A. S. Potdar, C. V. Rode, *RSC Adv.* **2015**, *5*, 16452–16460.  
[19] S. D. Lee, M. S. Park, D. W. Kim, I. Kim, D. W. Park, *Catal. Today* **2014**, *232*, 127–133.  
[20] M. B. Gawande, R. K. Pandey, R. V. Jayaram, *Catal. Sci. Technol.* **2012**, *2*, 1113–1125.  
[21] G. Parameswaram, M. Srinivas, H. Babu, P. S. S. Prasad, N. Lingaiah, *Catal. Sci. Technol.* **2013**, *3*, 3242–3249.  
[22] H. Li, D. Gao, P. Gao, F. Wang, N. Zhao, F. Xiao, W. Wei, Y. Sund, *Catal. Sci. Technol.* **2013**, *3*, 2801–2809.  
[23] S. Yuvaraj, W. Jong Lee, C. W. Lee, R. K. Selvan, *RSC Adv.* **2015**, *5*, 67210–67219.  
[24] M. B. Ali, F. B. Bouaifel, H. Elhouichet, B. Sieber, A. Addad, L. Boussekey, M. Ferid, R. Boukherroub, *J. Colloid Interface Sci.* **2015**, *457*, 360–369.

Received: October 5, 2015

Published online on December 9, 2015